Multipath-Enabled Super-Resolution for rf and Microwave Communication using Phase-Conjugate Arrays

Benjamin E. Henty* and Daniel D. Stancil†

Center for Wireless and Broadband Networking, Electrical and Computer Engineering Department, Carnegie Mellon University, Pittsburgh, Pennsylvania 15230, USA

(Received 31 July 2003; published 10 December 2004)

We demonstrate experimentally that phase-conjugate techniques can be used to achieve super-resolution focusing of electromagnetic waves in a multipath indoor environment at 2.45 GHz. The focusing phenomena was used to direct independent signals to two locations separated by approximately one-half wavelength, thereby creating two simultaneous channels at the same frequency. An increase in channel capacity is shown to be achievable by an experimental transmission of a 1 Mbps signal over two channels created using a four element phase-conjugate array.

DOI: 10.1103/PhysRevLett.93.243904 PACS numbers: 41.20.Jb, 42.25.Bs, 84.40.Ua

Introduction.—Electromagnetic waves propagating in both indoor and outdoor environments reflect and scatter from many objects, resulting in the creation of multiple paths from the transmitter to the receiver. Traditionally, this multipath propagation adversely affects the reliability and capacity of the wireless channel. However, recent research has focused on using these multiple propagation paths to enhance the radio channel. For example, it has been shown that if multiple transmit and receive antennas are used, multipath propagation can be exploited to realize multiple simultaneous information channels [1–3].

A novel approach to exploiting multipath for communications is time-reversal focusing [4,5]. Using ultrasonic waves in a water tank, Derode *et al.* [5] focused short pulses simultaneously at five spatially distinct locations using multipath propagation introduced intentionally by a randomly arranged forest of steel rods.

In this Letter we demonstrate that time-reversal focusing techniques can also be applied to electromagnetic waves at multigigahertz frequencies in indoor environments. In contrast to the acoustic measurements, our electromagnetic results involve signal bandwidths less than the coherence bandwidth and hence derive their focusing ability from multipath rather than bandwidth.

A time-reversed signal is represented in the frequency domain by the phase conjugate of the original signal. In addition to ultrasonics, phase-conjugate techniques have long been used in electromagnetics at both radio and optical frequencies. Phase-conjugate electromagnetic antenna arrays were developed in the early 1960s [6–8], and have been used extensively as retroreflective arrays. Van Atta [6] described a wideband technique in which symmetrically placed antennas in an array are connected by transmission lines that all exhibit the same time delay. A technique using nonlinear mixing with a locally generated radio frequency signal was introduced by Pon [7]. Nonlinear refraction techniques were developed in the 1970s to realize phase-conjugate optical mirrors [9,10].

The use of radio frequency retroreflecting arrays in multipath environments has recently begun to receive attention. Karode [11] discussed the use of phase-conjugate arrays as multipath sensors, and Tuovinen *et al.* [12] showed that radio links using a phase-conjugate array resulted in significantly less fading caused by multipath propagation. Even more recently, Lerosey *et al.* [13] demonstrated a time-domain technique for performing time reversal with electromagnetic waves. To the best of our knowledge, no one has previously demonstrated frequency-domain time-reversal super-resolution focusing with electromagnetic waves in multipath environments, nor demonstrated the potential for parallel channels via this focusing effect.

In this work we show that the focusing phenomenon can be realized with a bandwidth sufficient for significant rf communications to take place. This is an important result because it allows two users that are extremely close in space to use the same frequency band to communicate to the same array with significant isolation.

The electromagnetic time-reversal principle states that replacing t with $-t$ in any valid solution to Maxwell's equations results in a second valid solution, if the propagation environment is reciprocal. As an example, consider the fields from a source antenna that are completely characterized at a surface enclosing the source (it is sufficient to characterize the tangential components of the electric and magnetic fields). If sources are then placed at the surface and reproduce the characterized fields but with t replaced by $-t$, then a wave solution will be generated that propagates inward from the surface and focuses on the location of the original source antenna. This is the basic principle underlying time-reversal focusing.

In practice, a finite-size array antenna sparsely and incompletely measures the fields radiated by the source antenna. Consequently, the time-reversed signal retransmitted from the array will not precisely reproduce the time-reversed signal from the source antenna. However,

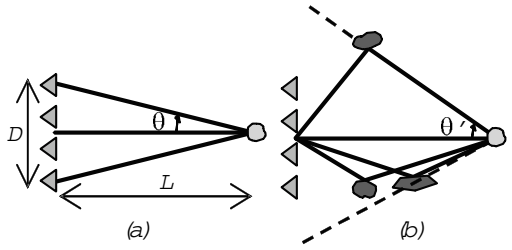

FIG. 1. (a) Graphic representation of numerical aperture of an antenna array, and (b) the enhancement of numerical aperture of an antenna array via salutary use of multipath.

the signals from the array elements that do arrive at the location of the original source antenna will be phased such that they interfere constructively, resulting in a localized region of increased field intensity. Since the fields from the array elements combine coherently at the target location and randomly elsewhere, the ratio of the amplitude at the focus to the surrounding values increases as $\sqrt{N}$ where N is the number of antenna array elements.

In our work, the term "super-resolution" is used to refer to an improved spatial focusing of power from an antenna beyond what is predicted by the Rayleigh criterion (i.e., cross-range focusing) and the depth of focus (i.e., range focusing). The Rayleigh criterion states that the minimum resolution is limited by $\frac{0.6\lambda}{\mathrm{NA}}$ where λ is the rf wavelength, $\mathrm{NA} = \sin\theta$ is the numerical aperture, and θ is the half angle subtended by the array as viewed from the target antenna, as shown in Fig. 1(a). Thus, it can be seen from Fig. 1(b) that an increase in scatterers in the environment allows an increase in the effective numerical aperture of the antenna array. However, the minimum size of the focused spot is of order $\frac{\lambda}{2}$.

Experimental setup.—Our measurements were conducted using a phase-conjugate, frequency-domain technique rather than a record and playback, time-domain technique. The experiments were conducted in a cluttered laboratory setting, as shown in Fig. 2. A four element antenna array was used to focus power at a target antenna. The array consisted of four panel antennas with 9 dBi of gain across the 2.4 to 2.5 GHz frequency band. A broadband discone antenna with an approximate gain of 2 dBi was used as the target antenna. To ensure that no line of site path was present, a large metal plate was placed about 1 m in front of the antenna array.

Power splitters and matched length cables were used to feed each array element with matched magnitude and phases, as shown in Fig. 3. A Herley Farmingdale 7122 vector modulator was used with each element to provide magnitude and phase shifts. The modulator is bidirectional and multiplies the rf signals passing through the modulator in either direction by a complex exponential, $Ae^{j\theta}$. The modulators are calibrated to provide amplitude coefficients, A, ranging from 0 to -70 dB and phase

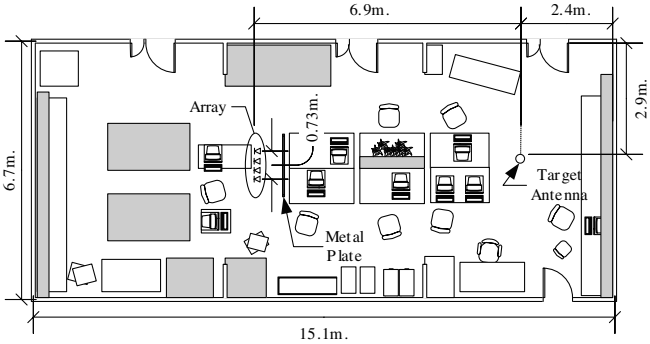

FIG. 2. Schematic of laboratory in which experiments were performed. Note the significant amount of clutter and the metal plate obstructing the line-of-sight path. All furniture and the metal plate were removed in the empty lab case.

shifts, θ, of 0 to 360° with an accuracy of ± 0.2 dB and $\pm 5°$ over the frequency and complex exponential ranges used in the experiment.

A vector network analyzer (VNA), shown in Fig. 3, was used to measure the magnitude and phase of the frequency response between the antenna array and target antenna. To perform the time reversal, the network analyzer was first configured to measure the reverse channel, from the target antenna to each of the array antenna elements, as follows. All modulators except one were set to the maximum attenuation value (> 70 dB) and a single modulator was set with the minimum attenuation and 0° phase shift. The VNA then measured the magnitude and phase response of the channel from the target antenna to the antenna array element at 2.45 GHz. This procedure was repeated for each array element. The measured magnitudes and phases were then normalized to the array element with the highest gain and the time-reversal (i.e., phase-conjugate) settings were computed. These settings were applied to each of the modulators to complete the time reversal. All signals sent through the modulators with these settings were thus transmitted with a phase conjugate to that of the channel.

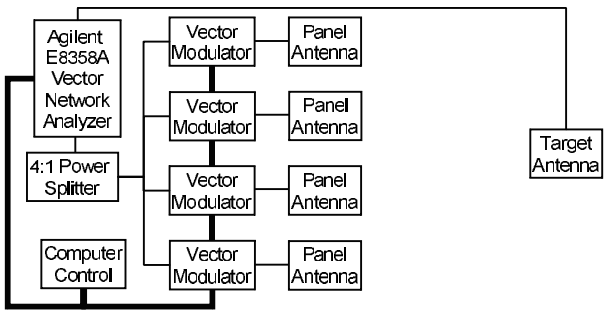

FIG. 3. Setup of apparatus for experiment. All cables were matched lengths. The vector network analyzer can be switched internally to measure from the target antenna to the array or vice versa.

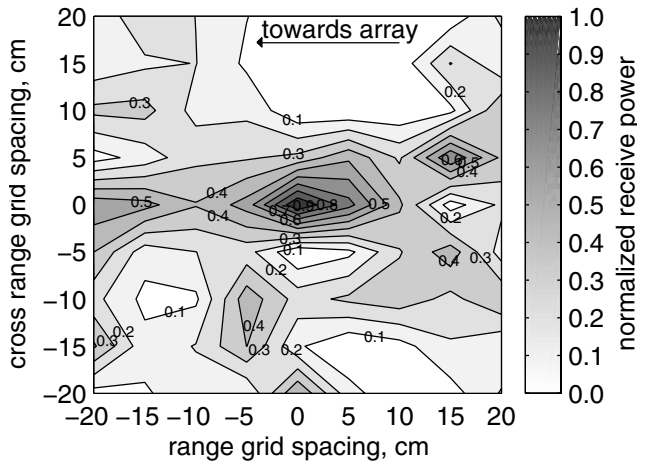

FIG. 4. Normalized, received power as measured in the area around the target location. Measurements were made manually every 5 cm at 81 grid points.

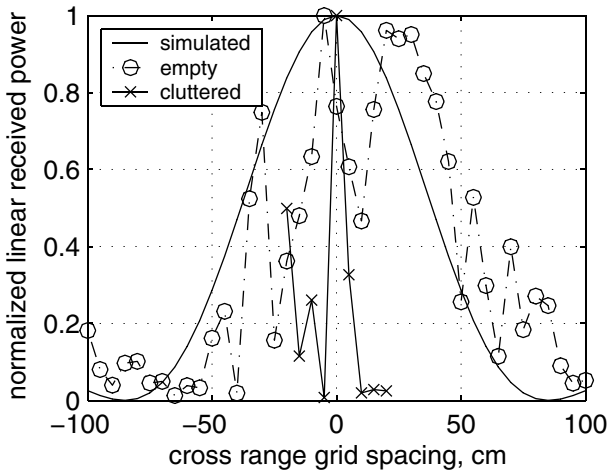

FIG. 5. Comparison of the cross-range focusing in the empty and cluttered lab measurements. In addition, the calculated focusing in an ideal multipath free setup is shown. The full widths at half maximum for the curves are as follows: simulated, 77 cm; empty, 90 cm; cluttered, 6 cm.

After the complex coefficients are applied to the vector modulators, the VNA was used to measure the channel response by recording the frequency response in the forward direction, from the antenna array to the target antenna (although, by reciprocity, the channel is independent of whether the target is the transmit or receive antenna). The amplitude received by the target antenna was measured at 81 points arranged in a square grid with 5 cm spacings and aligned manually via plumb bob with an estimated precision of ± 0.5 cm.

A contour plot generated from the measurements is shown in Fig. 4. The figure clearly shows the spatial focusing that results from the time-reversal antenna array. From the figure, the cross-range null-null width of the focused spot is about 12 cm. For comparison, the Rayleigh criterion for one-dimensional focusing reduces to $\sim 1.5\frac{L\lambda}{D}$. With $\lambda = 12.2$ cm, $L = 6.7$ m, and $D = 0.73$ m, the null-null spot size is 1.73 m, or over 10 times larger than the measured spot.

The result is even more striking in the range focusing direction. Figure 4 shows the spot size in the range direction to be about 25 cm, or roughly two wavelengths. The classical depth of focus for the array with line-of-sight and no multipath is $\sim 2\lambda(L/D)^2 = 20$ m, or roughly 80 times larger than the measured spot.

To better compare the measured focusing, the above measurements were repeated in the same room, but with all of the furniture and the metal plate removed. In addition, flat surfaces behind the target antenna were covered with rf absorbing material. This enabled a practical measurement of a setup in which the direct, free-space path significantly dominated the received signal, with comparatively minor multipath contributions. In this empty lab case, a cross-range measurement was made again in 5 cm steps, covering a range of 1 m to either side of the target location. The results are shown in Fig. 5 with the measurements from the cluttered case, as extracted from the data shown in Fig. 4. Also shown in Fig. 5 is the calculated focusing that is expected in a perfectly free-space scenario. By comparing this to the empty lab scenario, we see reasonable agreement with the size of the observed focused spot, considering some multipath scattering will be present in the nominally empty room. The deviation from a smooth curve is due to the remaining multipath that could not be suppressed without significant additional rf absorbing materials. We note that the multipath has a small bias in one direction so the focusing appears slightly offset from the center point.

Using the above techniques for focusing, two simultaneous communications channels were created. Four of the modulators in Fig. 6 were configured to focus on one target antenna location, and the other four were config-

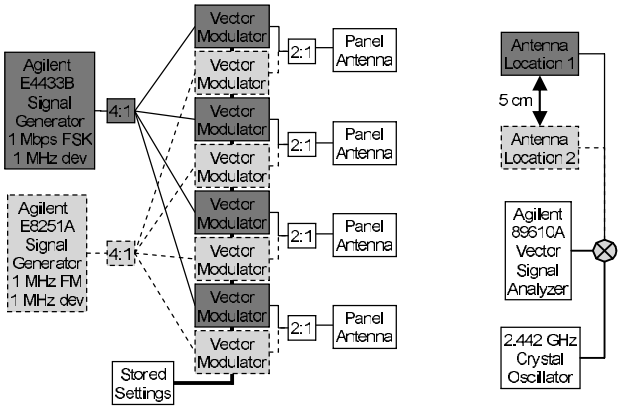

FIG. 6. Apparatus setup for bit error rate measurements of two phase-conjugate channels to two target locations separated by approximately 5 cm.

TABLE I. Measured channel isolation and resulting bit error rate in two phase-conjugate channels.

Environment	Channel	SIR	BER
Empty	1	1.9 dB	4.5%
Empty	2	0.2 dB	~50%
Cluttered	1	15.5 dB	0.1%
Cluttered	2	11.2 dB	2.2%

ured to focus on a target antenna location 5 cm away in the cross-range direction. The signals from each set of modulators were combined pairwise to drive the four elements in the array. This configuration created two simultaneous communication channels at the same frequency. The isolation between the two channels was found by comparing the amplitudes of the channels 1 and 2 signals at each antenna location. Signal to interference ratios (SIR) at the center frequency of focusing are reported in Table I.

To further characterize the viability for communications provided by the phase-conjugate enabled channels, a pseudonoise (PN) sequence, encoded via two tone frequency shift keying (FSK-2) was repeatedly transmitted at a one megabit per second (Mbps) rate. This test signal was transmitted using one phase-conjugate channel while an interfering 1 MHz, frequency modulated (FM) tone was transmitted at the same frequency on the second phase-conjugate channel. Both signals had a 1 MHz maximum frequency deviation and so occupied a nominal 2 MHz bandwidth about the center frequency used for the phase-conjugate focusing. The 50% correlation bandwidth in the cluttered environment was estimated to be approximately 14 MHz between 2.4 and 2.5 GHz.

A signal analyzer connected to the receive antenna at the focusing location of the intended channel demodulated and recorded the received bit stream. These bits were compared to the transmitted PN sequence to allow the bit error rate to be computed. This measurement was recorded for the first channel and then the FSK data signal was swapped with the FM signal to characterize the second phase-conjugate channel. This set of measurements was made in the empty lab and the cluttered lab scenario. The measured bit error rates (BER) are also shown in Table I. The reported BERs are high compared to an expected BER in the presence of an additive white Gaussian noise signal of the same power due to the similarity of the interfering signal to the transmitted signal. It should be noted that in the baseline case of the interfering FM signal turned off, the bit error rate was less than 10^{-4}, and in the case of both signals turned on but no phase-conjugate coefficients applied, the bit error rate was approximately 50%.

It is interesting to note that for the narrow-band case discussed here, the time-reversal technique naturally yields the optimum coefficients for adaptive beam-forming used with smart antennas [14]. Thus, in the presence of multipath, adaptive beam-forming techniques should result in super-resolution focusing.

In conclusion, we have shown that time-reversal focusing techniques in a multipath rich environment can be used to achieve focused spots that are more than an order of magnitude smaller in the cross-range direction than would be possible in a line-of-sight configuration without multipath, and almost 2 orders of magnitude smaller in the range direction. Using the focusing technique, two communications channels were established using a four element phase-conjugate array. These channels had sufficient signal isolation in a multipath environment to allow minimal bit error rates for a 2 MHz wide signal. Only one channel was achievable in the minimum multipath environment. Thus, this technique is promising for rf communications with increased capacity.

We acknowledge helpful discussions with Professor J. Moura, Professor J.-G. Zhu, and Professor R. Negi. This material is based in part upon work supported by the National Science Foundation under Grant No. 0219278 and by the Defense Advanced Research Project Agency under Grant No. W911NF-04-1-0031 administered by the Army Research Office.

*Electronic address: henty@eirp.org
†Electronic address: stancil@cmu.edu

[1] G. J. Foschini and J. J. Gans, Wirel. Pers. Commun. **6**, 311 (1998).
[2] E. Telatar, Eur. Trans. Telecommun. **10**, 585 (1999).
[3] A. L. Moustakas, H. U. Baranger, L. Balents, A. M. Sengupta, and S. H. Simon, Science **287**, 287 (2000).
[4] M. Fink, Sci. Am. **281**, No. 5, 91 (1999).
[5] A. Derode, A. Tourin, J. de Rosny, M. Tanter, S. Yon, and M. Fink, Phys. Rev. Lett. **90**, 014301 (2003).
[6] L. C. V. Atta, U.S. Patent No. 2908002: Electromagnetic Reflector, 1959.
[7] C. Y. Pon, IEEE Trans. Antennas Propag. **12**, 176 (1964).
[8] R. Y. Miyamoto and T. Itoh, IEEE Microw. Mag. **3**, 71 (2002).
[9] A. Yariv and D. M. Pepper, Opt. Lett. **1**, 16 (1977).
[10] D. M. Pepper, Sci. Am. **254**, No. 1, 74 (1986).
[11] S. L. Karode and V. F. Fusco, IEEE Microw. Guid. Wave Lett. **7**, 399 (1997).
[12] J. Tuovinen, G. S. Shiroma, W. E. Forsyth, and W. A. Shiroma, IEEE MTT-S Int. Microw. Symp. Dig. **3**, 1681 (2003).
[13] G. Lerosey, J. de Rosny, A. Tourin, A. Derode, G. Montaldo, and M. Fink, Phys. Rev. Lett. **92**, 193904 (2004).
[14] J. L. T. Litva and T. K.-Y. Lo, *Digital Beamforming in Wireless Communications* (Artech House, Boston, 1996), Chap. 3.